Published in final edited form as:
Retina. 2014 July ; 34(7): 1391–1399. doi:10.1097/IAE.0000000000000070.

THE VALUE OF RETINAL IMAGING WITH INFRARED SCANNING LASER OPHTHALMOSCOPY IN PATIENTS WITH STARGARDT DISEASE

Robert Chun, OD[*], **Gerald A. Fishman, MD**[*,†], **Frederick T. Collison, OD**[*], **Edwin M. Stone, MD, PHD**[‡,§], **Jana Zernant, MS**[¶], and **Rando Allikmets, PhD**[¶]

[*]Pangere Center for Inherited Retinal Disease, The Chicago Lighthouse For People Who Are Blind or Visually Impaired, Chicago, Illinois

[†]Department of Ophthalmology, University of Illinois, Chicago, Illinois

[‡]Howard Hughes Medical Institute, Chevy Chase, MD

[§]Department of Ophthalmology and Visual Sciences, University of Iowa Carver College of Medicine, Iowa City, Iowa

[¶]Department of Ophthalmology, Columbia University, New York, New York

Abstract

Purpose—To demonstrate the value of infrared scanning laser ophthalmoscopy (SLO) for determining structural retinal and choroidal changes in patients with Stargardt disease and its comparison to findings on short-wavelength fundus autofluorescence (SW-AF) imaging, spectral-domain optical coherence tomography, and microperimetry measurements.

Methods—Forty-four eyes of 22 patients with Stargardt disease were studied using infrared-SLO, spectral-domain optical coherence tomography, macular microperimetry, SW-AF, electroretinography, and fundus photography.

Results—Although SW-AF imaging outlined the regions of retinal pigment epithelial (RPE) atrophy (hypofluorescence) and enhanced the visibility of more funduscopically apparent flecks (hyperfluorescence), infrared-SLO imaging outlined the regions of choroidal, and RPE, atrophic changes. Degenerative changes in photoreceptor and RPE cell layers, evident on spectral-domain optical coherence tomography imaging, were associated with either hyporeflective or hyperreflective images on infrared-SLO imaging, depending on whether both RPE and choroidal atrophy (hyperreflectance) or solely RPE atrophy (hyporeflectance) was present. Threshold elevations on microperimetry testing corresponded to both RPE and choroidal atrophy on infrared-SLO imaging and RPE atrophy on SW-AF.

Conclusion—Although SW-AF identifies regions of RPE atrophy, infrared-SLO also identifies the involvement of the choroid that has important implications for the potential improvement in

Reprint requests: Gerald A. Fishman, MD, Pangere Center for Inherited Retinal Disease, The Chicago Lighthouse For People Who Are Blind or Visually Impaired, 1850 West Roosevelt Road, Chicago, IL 60608; gerafish@uic.edu.

None of the authors have any financial/conflicting interests to disclose.

visual function from treatment. Thus, infrared-SLO imaging offers an additional advantage beyond that obtained with SW-AF.

Keywords

infrared-SLO imaging; microperimetry; short-wavelength autofluorescence; Stargardt disease

Stargardt disease is a recessively inherited form of macular dystrophy that predominantly causes loss of central vision in approximately 1 in 8,000 to 1 in 10,000 people in the United States.[1] Although it is commonly associated with a juvenile onset, patients may present into adulthood. Described by Karl Stargardt in 1909, the characteristic findings of Stargardt disease include the presence of yellow flecks in the macula or throughout the posterior pole of the fundus.[2,3] Patients with Stargardt disease may present with or without an atrophic-appearing macular lesion depending on the level of severity of the disease and can be classified according to the distribution and stage of their fundus flecks.[3] Other classification systems exist, including one involving the degree of functional loss using electrophysiologic testing.[4]

With the emergence of Stargardt treatment trials, it has become of paramount importance to identify sensitive measurements of retinal structure and function that can be used as effective clinical outcome measures. In Stargardt disease, noninvasive retinal imaging, with infrared scanning laser ophthalmoscopy (SLO) and short-wavelength autofluorescence (SW-AF) technology, has allowed for improved visualization of disease-related fundus changes that may be otherwise difficult to see funduscopically. The development of spectral-domain optical coherence tomography (SD-OCT) coupled with infrared-SLO imaging offers confocal and cross-sectional analyses of the retina, allowing an improved clinical assessment of patients with Stargardt disease.[5] Additionally, functional testing, made possible with microperimetry (MP), facilitates a comparison with structural retinal abnormalities.

In this study, patients with Stargardt disease were evaluated using infrared-SLO imaging, SD-OCT, SW-AF, macular MP, fundus photography, and full-field electroretinograms (ERG). We compared the structural abnormalities seen on infrared-SLO with those observed with SW-AF and SD-OCT, identifying any possible redundancy in the use of these imaging modalities or potentially different information provided by each test. Associations of each test were also made with functional measurements obtained by macular MP.

Methods

Subjects

Twenty-two patients with Stargardt disease were included in the study. Their age ranged from 21 years to 60 years with a mean age of 39 ± 11 years. A written informed consent was obtained in accordance with the Declaration of Helsinki and the American Health Insurance Portability and Accountability Act (HIPAA). The study was approved by the Institutional Review Board of the University of Illinois at Chicago.

If no disease causing mutation was found by genetic analysis, a clinical diagnosis was confirmed by an expert in Stargardt disease based on the ocular history of visual loss, psychophysical testing, including visual fields, and characteristic retinal findings (Subjects 2, 6, 12, and 22). These patients represented varying phenotypes based on the distribution of their fundus flecks according to a previously described classification system.[3] Stage 1 disease indicated flecks limited to the macula with or without the presence of an atrophic macular lesion. In Stage 2 disease, the flecks were distributed throughout the posterior pole and located anterior to the vascular arcades. In Stage 3, the flecks were diffusely resorbed with, not infrequently, choriocapillaris atrophy within the macula. Stage 4 patients showed very advanced Stargardt disease in which there was diffuse choroidal and retinal pigment epithelial (RPE) atrophy throughout the fundus.

All patients were examined by biomicroscopy, applanation tonometry, and dilated funduscopy before the completion of SD-OCT, infrared-SLO, SW-AF, MP, and fundus photography. Of the 22 patients, 4 did not complete imaging with SW-AF. Full-field ERGs were completed on at least 1 eye in 15 of the 22 patients. Best-corrected visual acuity was obtained using an Early Treatment of Diabetic Retinopathy Study chart.

Instruments and Testing

Canon instrumentation (Melville, NY) was used to obtain 60° color fundus photographs of each eye after pupillary dilation. Infrared-SLO and SD-OCT imaging (using an 830 nm light), in addition to MP testing, were performed using OPTOS instrumentation (Marlborough, MA), formerly OPKO instrumentation (Miami, FL). Images of SW-AF (using a 488 nm light) were obtained using a confocal scanning laser ophthalmoscope of Heidelberg Engineering (Heidelberg, Germany). The technical details of retinal imaging with the OPTOS and Heidelberg devices were previously described.[5–7]

For SW-AF, images were obtained on 2 gain settings at 85 and 95.[6] The image quality varied between each gain level. Those SW-AF images that highlighted the fundus most effectively were included in the study.

For MP measurements, patients were asked to maintain fixation on a central white cross subtending 3.3°. The nontested eye was occluded throughout the test. Achromatic stimuli (Goldmann Size III target with 200-millisecond duration) were consecutively presented on a 10 cd/m^2 white background using a 4 to 2 threshold strategy. A pattern grid, termed Polar 3, was used to test 28 macular points arranged in 3 concentric circles (2.3°, 6.6°, and 11°, respectively, in diameter).[5,8] Patients with stable foveal fixation were asked to locate the central target, allowing the Polar 3 to be centered in the central macula. Patients with eccentric viewing or unsteady fixation were asked to locate the white cross, and the pattern grid was manually centered in the macula to allow for accurate testing of the central macular region. In addition, a manual pattern was subsequently used based on the characteristics of the infrared-SLO retinal image, using points outside the 11° diameter of the Polar 3 pattern.

Threshold values on MP were evaluated with respect to infrared-SLO and SW-AF images. Because SW-AF imaging was completed using a different instrument than MP testing, threshold sensitivity results had to be superimposed on SW-AF images for each patient

using custom software written in Matlab (Natick, MA). Corresponding threshold sensitivities on MP testing that were superimposed on infrared-SLO and SW-AF images were indicated in decibels (dB). A value of 0 dB on MP (illustrated by an open, red circle in the region that was tested) represented a dense scotoma, indicating that the subject was unable to see the brightest test stimulus presented. A value of 16 dB to 20 dB was considered normal, 12 dB to 14 dB was mildly subnormal, 6 dB to 10 dB was moderately subnormal, and 4 dB or less was markedly subnormal on our instrument.[5,8]

Full-field ERGs were obtained using a Burian-Allen contact lens electrode and the Diagnosys ColorDome (Diagnosys LLC, Lowell, MA). Testing conformed to the standards set by the International Society for Clinical Electrophysiology of Vision with the exception to using a 4.5 cd-s/m^2 achromatic stimulus for the photopic single flash (cone isolating) and a 0.005 cd-s/m^2 blue stimulus for the scotopic dim single flash (rod isolating).[9] Results were evaluated based on a normative database using 90% tolerance limits.

Results

Of the total 22 patients studied, 7 (32%) were categorized as having Stage 1 Stargardt disease, 6 (27%) were Stage 2, and 9 (41%) were Stage 3. All 22 patients showed fundus flecks at one time. Flecks were not evident in four Stage 3 siblings on their most recent examination. Although parafoveal flecks were noted at the time of their diagnosis, they progressed to show severe RPE and choroidal atrophy throughout the posterior pole.

Genetic analysis was performed at the University of Iowa Carver Laboratory and at Columbia University, Department of Ophthalmology. The *ABCA4* gene was analyzed by direct sequencing on all patients (Table 1). The entire *ABCA4* gene was sequenced except for in 5 patients. At least 1 *ABCA4* mutation was found in 18 of the 22 patients (82%). No likely pathogenic *ABCA4* variants were found in four patients. For these patients, a clinical diagnosis of Stargardt disease was based on the history, examination, and retinal findings.

On infrared-SLO imaging, fundus flecks varied in reflectance intensity and appearance. Larger more funduscopically apparent flecks were hyperreflective, while reabsorbing flecks appeared hyporeflective (dark). Bright, hyperreflective areas either were associated with both RPE and choroidal atrophy (increasingly visible sclera) or funduscopically evident flecks. Dark, hyporeflective regions indicated resorbing or resorbed flecks with an intact choroid and corresponded to disrupted photoreceptor and RPE layers on OCT testing. Figure 1 includes images from Patient 10 with Stage 2 Stargardt disease and 20/25 visual acuity. A fundus photograph (Figure 1A) shows a bull’s eye–appearing macular lesion surrounded by a ring of parafoveal flecks. The SLO image (Figure 1B) includes a dark, hyporeflective parafoveal region that represents distinct areas of atrophic changes in the RPE.

However, SW-AF effectively outlined the regions of RPE atrophy indicated by dark, hypofluorescent regions. It enhanced areas of more funduscopically apparent flecks (Figure 1C). Some flecks appeared partially fluorescent (bright) or hypofluorescent (dark). Many flecks visualized with SW-AF were also easily visible on infrared-SLO imaging. However, in other instances, the flecks appeared relatively different when comparing images.

Findings of OCT associated with structural changes on infrared-SLO imaging were most evident among patients with a bull's eye–appearing macular lesion. Loss of the inner segment ellipsoid band[10] corresponded to a dark, disrupted area surrounding the fovea on the infrared-SLO image. Figures 1 and 2 show representative instances of a bull's eye–appearing macula with relative foveal sparing on OCT imaging (yellow arrows point to spared foveal regions of the inner segment ellipsoid). Figures 1F and 2F show the superimposed SD-OCT and infrared-SLO images that illustrate the parafoveal loss of the inner segment ellipsoid and disruption of RPE just outside the fovea (red arrows).

Within the same group of patients having a bull's eye–appearing macular lesion, the middle ring of MP results corresponded well to the parafoveal loss of the inner segment ellipsoid and disruption of the RPE noted on SD-OCT. Results from MP showed relatively more functional loss within this middle ring of points tested with the Pattern 3 grid, when compared with the inner or outer rings of the grid (Figures 1, D and E and 2, D and E). The severity of functional loss varied from 0 dB to 12 dB, where the reduction of sensitivities corresponded to the amount of structural loss apparent on SD-OCT, infrared-SLO, and SW-AF images. Areas with subtle signs of disruption seen on SLO and AF imaging showed less reduction in threshold sensitivities and were categorized as having more mildly subnormal (12–14 dB) or moderately subnormal (6–10 dB) function.

Threshold sensitivities on MP were found to correspond well with structural changes in patients having steady fixation with the absence of significant RPE and choroidal atrophy in the macula. Patients with 20/40 or better visual acuity showed preserved central foveal function in tested MP points with corresponding reduction in threshold sensitivities in areas of photoreceptor or RPE degeneration. In some instances, there were a few macular MP threshold sensitivities that did not always correspond with areas of marked atrophy on the infrared-SLO image. This variability and lack of functional correspondence was most apparent at the borders of marked atrophic lesions in the macula among patients with Stage 3 Stargardt disease.

In addition to the structural and functional associations mentioned, another significant finding from the study included the advantage of imaging with the infrared-SLO, given its ability to provide information about the choroid. In Figure 1A from Patient 10, the black arrow points to a lesion that could correspond to either a large resorbing fleck or an area of RPE atrophy on the fundus photograph. The SW-AF image confirmed that the lesion corresponded to an area of RPE atrophy (green arrow in Figure 1C). Infrared-SLO imaging additionally showed that the lesion in question was hyperreflective and thus confirmed that both the RPE and choroid were atrophic (blue arrow in Figure 1B). Without the presence of choriocapillaris and larger choroidal vessels to absorb infrared light, the incoming light is reflected by the sclera. Figure 3 vividly illustrates how the infrared-SLO imaging highlights the regions of choroidal vessel atrophy that would not have been disclosed had SW-AF imaging alone been obtained. There were two patients in the study who showed significant signs of RPE and choroidal atrophy within the macula but still retained favorable central vision because of relative preservation of foveal structure and function. Figure 3 includes a fundus photographs, infrared-SLO image, and a SW-AF image, respectively, of these two patients with 20/25 vision. The patient in the top row corresponds to Subject 17, whereas the

patient in the bottom row corresponds to Subject 22 (Table 1). Both patients demonstrate marked RPE and choroidal atrophy within the macula. Subject 17 shows a small island of foveal preservation that is evident both on the infrared-SLO (hyporeflectance) and SW-AF (hyperfluorescence surrounded by hypofluorescence) images and on the fundus photograph. In the same manner, the infrared-SLO and SW-AF images of Subject 22 (Figures 3, E and F) illustrate a finger-shaped area of the fovea that is preserved but surrounded by extensive RPE and choroidal atrophy.

Full-field ERGs were obtained on 4 patients with Stage 1 disease, 5 patients with Stage 2 disease, and 6 patients with Stage 3 disease. All 4 patients with Stage 1 Stargardt disease demonstrated normal rod and cone signals. Three of the 6 patients with Stage 2 disease showed borderline subnormal cone function but normal rod function. All 6 patients in the Stage 3 category showed a marked full-field ERG abnormality with subnormal rod and cone responses.

Discussion

The main goal of this study was to demonstrate the value of imaging with infrared-SLO and to illustrate the complementary roles of SW-AF, SD-OCT, and MP testing. It is evident that both infrared-SLO and SW-AF imaging provide more information about structural abnormalities than often is visible by funduscopy or fundus photography. However, SW-AF imaging can cause more discomfort for patients from the high-intensity short-wavelength light used (488 nm excitation) compared with infrared-SLO imaging. Furthermore, the cumulative effect of exposure to such light needs additional investigation.[10–12] Identifying the presence of atrophic choroidal changes on infrared-SLO imaging is an added advantage over the use of SW-AF. As noted in a previous study, it was also found that infrared-SLO imaging detected a greater area of retinal pigmentary abnormalities when compared with SW-AF imaging.[5] For these reasons, infrared-SLO imaging should be considered for use in monitoring the progression of Stargardt disease and when selecting patients for treatment trials.

The concentration and orientation of the melanosomes and lipofuscin within dysfunctional RPE cells may have contributed to the varied appearance of flecks (fluorescence and reflectance) on the confocal surface images of both the SW-AF and infrared-SLO imaging.[13] Although most funduscopically apparent flecks were equally visible on SW-AF and infrared-SLO images, the broadband absorption of melanin and the absorption characteristics of SW-AF versus infrared-SLO may be a reason for the varied relations when comparing individual fleck lesions from one imaging modality to another.

Besides infrared-SLO and SW-AF imaging, a full-field ERG may be another objective means for monitoring progression in patients with more advanced Stargardt disease. Patients with more diffuse retinal changes observed by infrared-SLO and SW-AF imaging were those who consistently demonstrated subnormal ERG responses in cone and rod function.

Microperimetry was an effective means to quantify macular visual function, mainly in patients with steady fixation and less severe Stargardt disease. Cideciyan et al[14] reported

indications of variability in test–retest repeatability at the border of deep scotomas in patients with *ABCA4* disease. It was also noted by Sunness and Steiner[15] that there was a lack of association between the structure and function between the loss of autofluorescence and the precise size and location of scotomas measured with MP in patients with geographic atrophy. Overall, the MP results in our study corresponded well when the structure was preserved on SD-OCT testing and when threshold sensitivities were evaluated away from the borders of atrophic macular lesions.

In summary, infrared-SLO imaging can provide additional structural information of the retina beyond that obtained by SW-AF imaging. The degree of structural changes on SLO imaging is associated with elevations of visual thresholds on MP and structural changes determined by SD-OCT imaging.

Acknowledgments

Supported by the Pangere Corporation, Grousbeck Family Foundation, Stanford, CA, Cless Family Foundation, Northbrook, IL, Wynn-Gund Foundations, and in part by the National Eye Institute/National Institutes of Health grants (EY021163, EY019861) and Foundation Fighting Blindness (Owings Mills, MD).

References

1. Blacharski, PA. Fundus flavimaculatus. In: Newsome, DA., editor. Retinal Dystrophies and Degenerations. New York, NY: Raven Press; 1988. p. 135-159.
2. Stargardt K. Ueber familiar, progressive Degeneration in der Makulagegend des Auges, Graefe. Arch Ophthalmol. 1909; 71:534.
3. Fishman GA. Fundus flavimaculatus. A clinical classification. Arch Ophthalmol. 1976; 94:2061–2067. [PubMed: 999551]
4. Lois N, Holder GE, Bunce C, et al. Phenotypic subtypes of Stargardt macular dystrophy-fundus flavimaculatus. Arch Ophthalmol. 2001; 119:359–369. [PubMed: 11231769]
5. Anastasakis A, Fishman GA, Lindeman M, et al. Infrared scanning laser ophthalmoscope imaging of the macula and its correlation with functional loss and structural changes in patients with Stargardt disease. Retina. 2011; 31:949–958. [PubMed: 21293320]
6. Hassenstein A, Meyer CH. Clinical use and research applications of Heidelberg retinal angiography and spectral-domain optical coherence tomography—a review. Clin Experiment Ophthalmol. 2009; 37:130–143. [PubMed: 19338610]
7. Schmitz-Valckenberg S, Holz FG, Bird AC, Spaide RF. Fundus autofluorescence imaging: review and perspectives. Retina. 2008; 28:385–409. [PubMed: 18327131]
8. Anastasakis A, McAnany JJ, Fishman GA, Seiple WH. Clinical value, normative retinal sensitivity values, and intrasession repeatabiliity using a combined spectral domain optical coherence tomography/scanning laser ophthalmoscope microperimeter. Eye. 2011; 25:245–251. [PubMed: 21178993]
9. Marmor MF, Fulton AB, Holder GE, et al. ISCEV standard for clinical electroretinography (2008 update). Doc Ophthalmol. 2009; 118:69–77. [PubMed: 19030905]
10. Spaide RF, Curcio CA. Anatomical correlates to the bands seen in the outer retina by optical coherence tomography: literature review and model. Retina. 2011; 31:1609–1619. [PubMed: 21844839]
11. Cideciyan AV, Swider M, Aleman TS, et al. Reduced-illuminance autofluorescence imaging in ABCA4-associated retinal degenerations. J Opt Soc Am A Opt Image Sci Vis. 2007; 24:1457–1467. [PubMed: 17429493]
12. Morgan JI, Hunter JJ, Masella B, et al. Light-induced retinal changes observed with high-resolution autofluorescence imaging of the retinal pigment epithelium. Invest Ophthalmol Vis Sci. 2008; 49:3715–3729. [PubMed: 18408191]

13. Duncker T, Tabacaru MR, Lee W, et al. Comparison of near-infrared and short-wavelength autofluorescence in retinitis pigmentosa. Invest Ophthalmol Vis Sci. 2013; 54:585–591. [PubMed: 23287793]

14. Cideciyan AV, Margozata S, Tomas SA, et al. Macular function in macular degenerations: repeatability of microperimetry as a potential outcome measure for ABCA4-associated retinopathy trials. Invest Ophthalmol Vis Sci. 2012; 53:841–852. [PubMed: 22247458]

15. Sunness JS, Steiner JN. Retinal function and loss of autofluorescence in Stargardt disease. Retina. 2008; 28:794–800. [PubMed: 18536594]

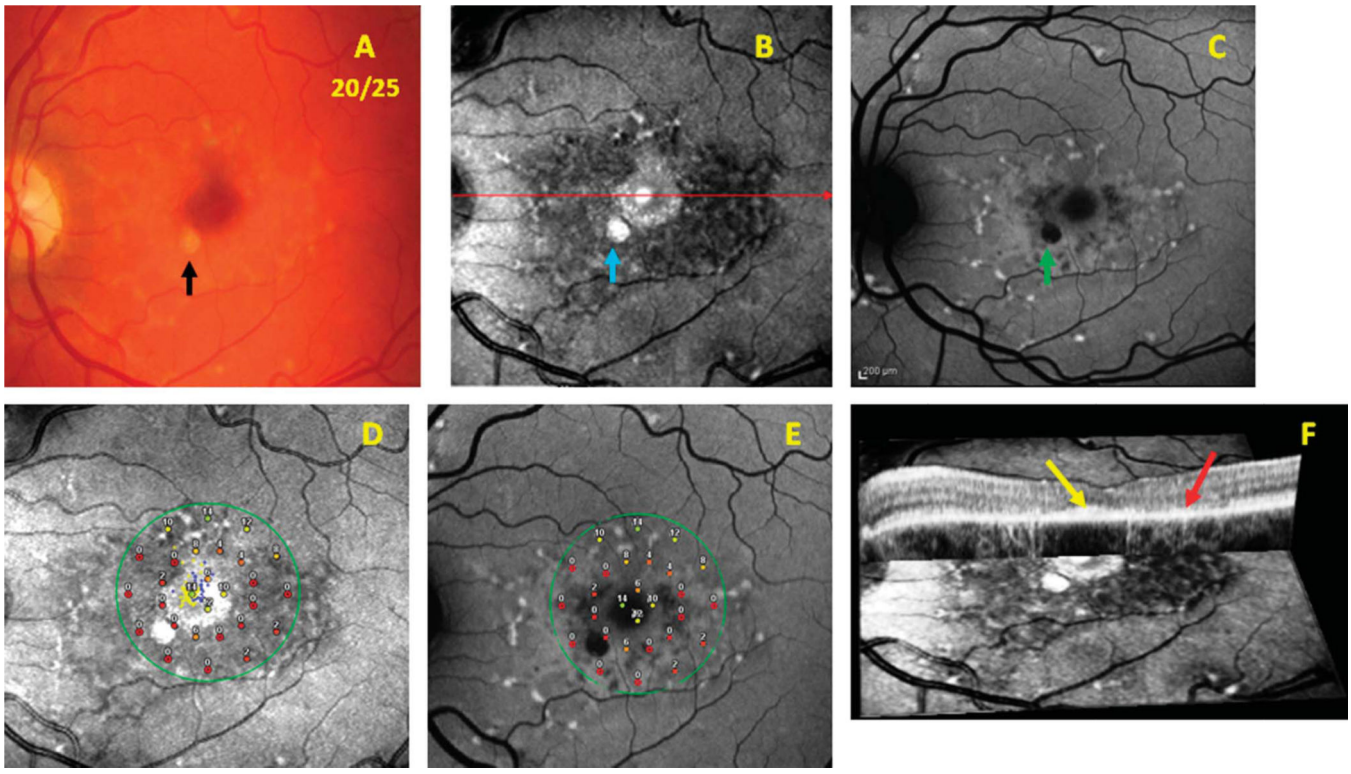

Fig. 1.

Patient 10. Images from a patient with Stage 2 Stargardt disease comparing results from the infrared-SLO, SW-AF, SD-OCT, and MP testing. **A**. Color fundus photograph. **B**. Infrared-SLO image. **C**. Short-wavelength fundus autofluorescence image. **D**. Results from MP superimposed on an infrared-SLO image. **E**. Results from MP superimposed on a SW-AF image. **F**. Cross-sectional OCT image superimposed on the surface of an infrared-SLO image.

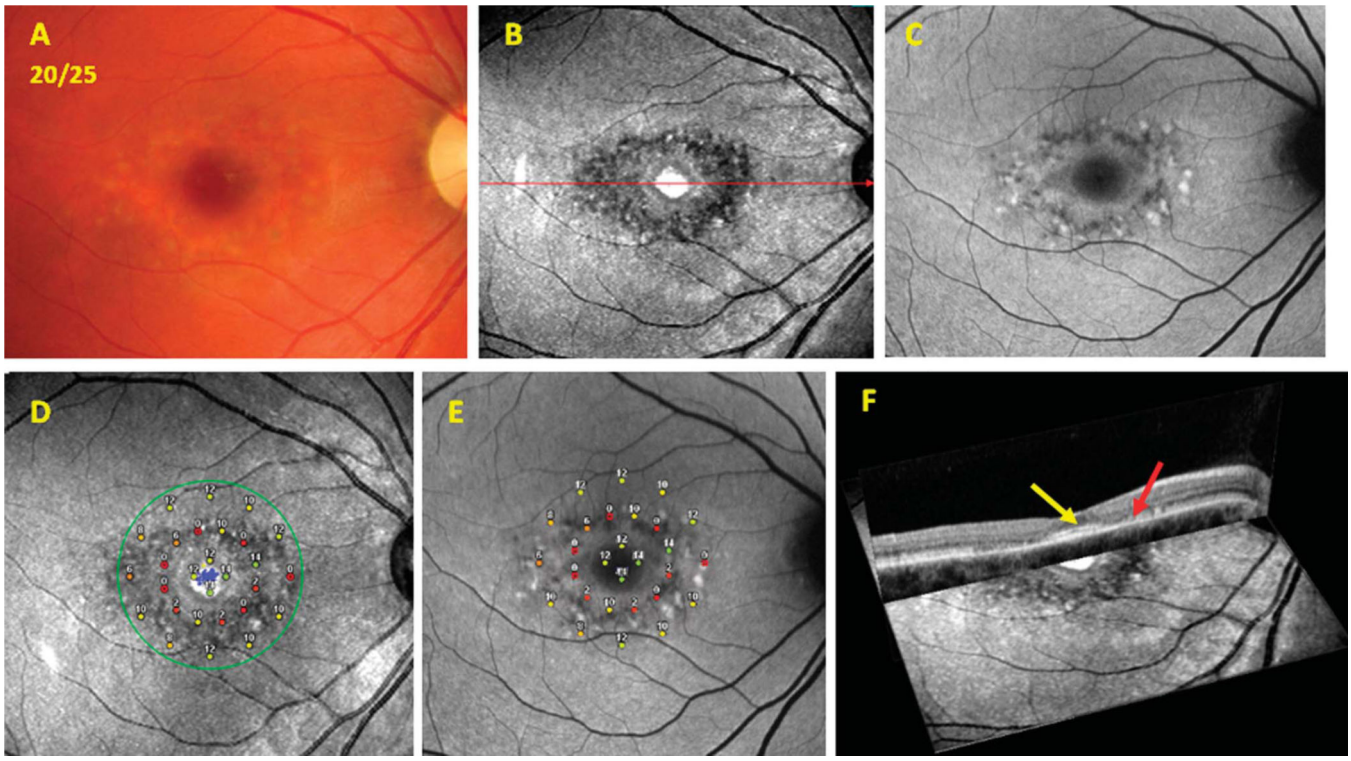

Fig. 2.

Patient 7. Images from a patient with Stage 2 Stargardt disease comparing results from the infrared-SLO, SW-AF, SD-OCT, and MP testing. **A**. Color fundus photograph. **B**. Infrared-SLO image. **C**. Short-wavelength fundus autofluorescence image. **D**. Results from MP superimposed on an infrared-SLO image. **E**. Results from MP superimposed on a SW-AF image. **F**. Cross-sectional OCT image superimposed on the surface of an infrared-SLO image.

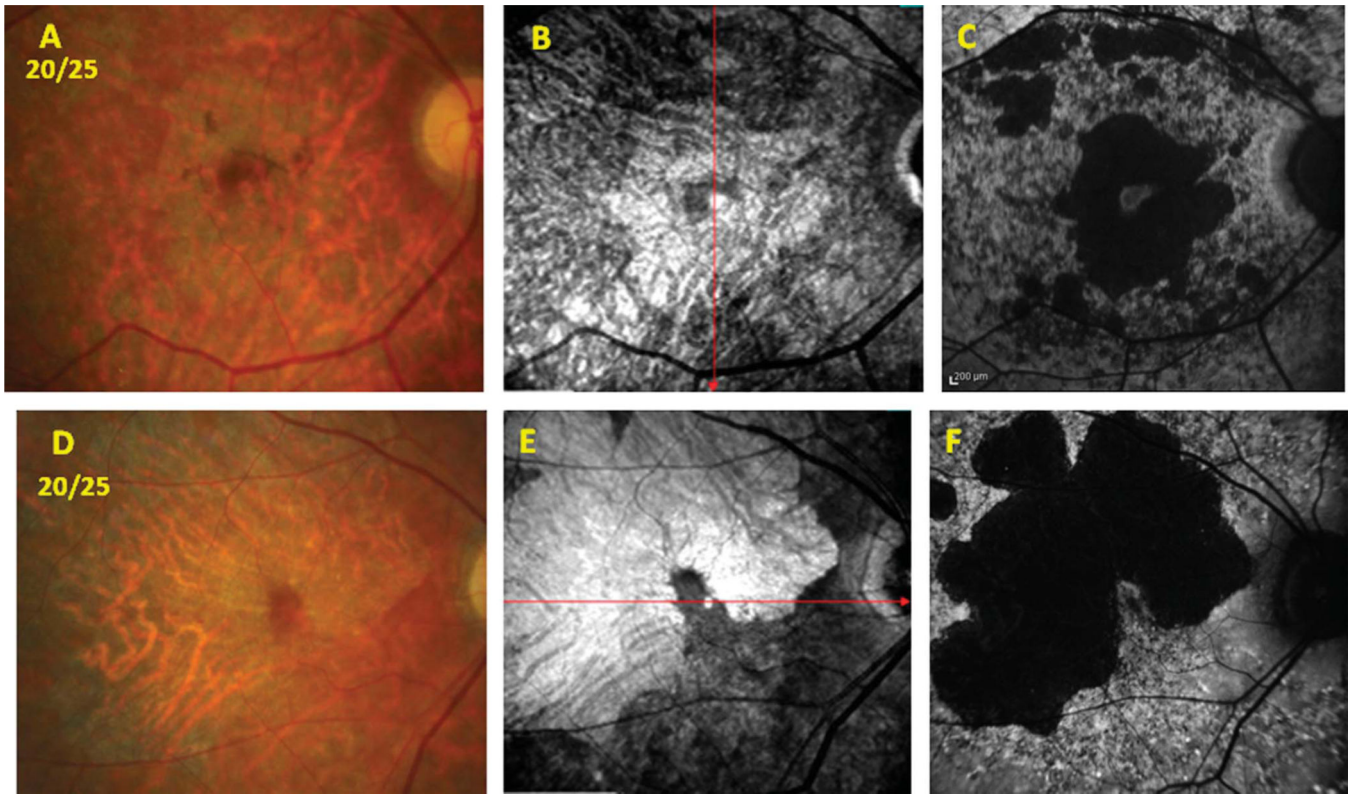

Fig. 3.

Patients 17 and 22. Images comparing the infrared-SLO and SW-AF results that localize areas of RPE and choroidal atrophy in 2 patients with Stage 3 Stargardt disease with 20/25 vision. **A** to **C.** Patient 17. **A**. Color fundus photograph. **B**. Infrared-SLO image. **C**. Short-wavelength fundus autofluorescence image. **D** to **F** Patient 22. **D**. Color fundus photograph. **E**. Infrared-SLO image. **F**. Short-wavelength fundus autofluorescence image.

Table 1

Summary of Patient Demographics and Clinical Findings Confirming Diagnosis

Subject	Sex/Age	Stage	BCVA (OD, OS)	Fundus Findings	Disease-Associated Variants in *ABCA4*	Full-Field ERG
1	F/31	1	20/125, 20/125	OU: Atrophic macular lesion with parafoveal flecks	Heterozygous: Q636X	Normal rod, normal cone
2	F/41	1	20/25, 20/40	OU: Bull's eye–appearing lesion with parafoveal flecks	No mutation found	Normal rod, normal cone
3	F/45	1	20/25, 20/20	OU: Bull's eye–appearing lesion with parafoveal flecks	Compound heterozygous: I975M and K1978E	—
4*	M/21	1	20/40, 20/40	OU: Bull's eye–appearing lesion with parafoveal flecks	Compound heterozygous: R219T, W439X, and G863A	Normal rod, normal cone
5*	F/23	1	20/30, 20/20	OU: Bull's eye–appearing lesion with parafoveal flecks	Compound heterozygous: R219T, W439X, and G863A	—
6	F/32	1	20/80, 20/125	OU: Bull's eye–appearing lesion with parafoveal flecks	No mutation found	—
7	F/30	1	20/25, 20/25	OU: Bull's eye–appearing lesion with parafoveal flecks	Heterozygous: R2077W	Normal rod, normal cone
8	M/33	2	20/125, 20/160	OU: Bull's eye–appearing lesion with flecks throughout posterior pole	Heterozygous: K2056X	Normal rod, normal cone
9	M/47	2	20/160, 20/40	OU: Bull's eye–appearing lesion with flecks throughout posterior pole	Heterozygous: E1087K	Normal rod, subnormal cone
10	F/42	2	20/25, 20/25	OU: Bull's eye–appearing lesion with flecks throughout posterior pole	Compound heterozygous: G550R and R2030Q	Normal rod, normal cone
11	F/32	2	20/200, 20/200	OU: Hyperpigmented atrophic macular lesion with flecks throughout posterior pole	Heterozygous: IVS38-10 T>C	Normal rod, subnormal cone
12	F/21	2	20/160, 20/160	OU: Atrophic RPE changes in macula with flecks throughout the posterior pole	No mutation found	Normal rod, subnormal cone
13	F/60	2	20/20, 20/20	OU: No evidence of an atrophic lesion in the fovea, diffuse flecks throughout posterior pole, fundus flavimaculatus phenotype	Compound heterozygous: G1961E and G1532N	—
14	F/34	3	20/200, 20/250	OU: Severe RPE and choroidal atrophic changes in macula and throughout posterior pole and midperiphery, flecks throughout posterior pole	Compound heterozygous: G818E and C1488R	Subnormal rod, subnormal cone
15	M/47	3	20/64, 20/125	OU: Atrophic macular lesion with relative foveal sparing, flecks throughout posterior pole	Compound heterozygous: G863A and IVS1-2A>G	—
16*	M/40	3	20/200, 20/160	OU: Severe RPE and choroidal atrophic changes in macula and throughout posterior pole and midperiphery, parafoveal flecks at onset	Compound heterozygous: IVS38-10 T>C and IVS40+5 G>A	Subnormal rod, subnormal cone
17	M/53	3	20/25, 20/32	OU: Marked RPE and choroidal atrophic changes in the macula with relative foveal sparing, resorbing flecks apparent throughout posterior pole	Heterozygous: G1975R	—
18*	F/53	3	20/200, 20/250	OU: Severe RPE and choroidal atrophic changes in macula and throughout posterior pole and midperiphery, parafoveal flecks at onset	Compound heterozygous: IVS38-10 T>C and IVS40+5 G>A	Subnormal rod, subnormal cone

Subject	Sex/Age	Stage	BCVA (OD, OS)	Fundus Findings	Disease-Associated Variants in *ABCA4*	Full-Field ERG
19*	M/50	3	20/160, 20/250	OU: Severe RPE and choroidal atrophic changes in macula and throughout posterior pole and midperiphery, parafoveal flecks at onset	Compound heterozygous: IVS38-10 T>C and IVS40+5 G>A	Subnormal rod, subnormal cone
20	F/34	3	20/160, 20/160	OU: Bull's-eye appearing lesion with flecks throughout posterior pole	Compound heterozygous: L541P, A1038V, and D576H	Subnormal rod, subnormal cone
21*	M/39	3	20/250, 20/250	OU: Severe RPE and choroidal atrophic changes in macula and throughout posterior pole and midperiphery, parafoveal flecks at onset	Compound heterozygous: IVS38-10 T>C and IVS40+5 G>A	—
22	M/60	3	20/20, 20/20	OU: Marked RPE and choroidal atrophic changes in the macula and throughout posterior pole with relative foveal sparing, few residual fundus flecks apparent	No mutation found	Subnormal rod, subnormal cone

M, male; F, female; OD, right eye; OS, left eye; OU, both eyes; BCVA, best-corrected visual acuity.

*Same family.